Inter-Relay Cooperation: A New Paradigm for Enhanced Relay-Assisted FSO Communications

Chadi Abou-Rjeily, *Senior Member IEEE*, and Serj Haddad

***Abstract*—In this paper, we study the effect of the presence of inter-relay connections on the performance of cooperative free-space optical (FSO) networks. Unlike the existing literature where conventional cooperation in FSO systems is realized in two steps through source-relay (S-R) followed by relay-destination (R-D) communications, we propose and analyze a novel three-stage cooperation methodology. The proposed scheme is based on exploiting the potential presence of FSO links between neighboring relays for the sake of complementing the S-R and R-D steps with an intermediate inter-relay communication step that serves in enhancing the fidelity of signal reconstruction at the relays before retransmitting to the destination. For the proposed scheme, we derive closed-form expressions for the conditional error probability with any number of relays. We also propose a closed-form power allocation strategy (PAS) in the case where the background noise is negligible. This PAS is based on minimizing an asymptotic upper-bound on the conditional error probability by applying the method of Lagrange multipliers with the solution satisfying the Karush-Kuhn-Tucker (KKT) conditions. Results show that the presence of inter-relay connections, associated with an appropriate cooperation scheme and PAS, can significantly boost the performance of relay-assisted FSO systems.**

***Index Terms*—Free-space optics, FSO, cooperation, relay, cooperative diversity, spatial diversity, fading channels.**

I. Introduction

Recently, there has been a growing interest in Free-Space Optical (FSO) communications as an attractive and cost-effective solution to the "last mile" problem [1]. The nature of propagation of optical signals through the atmosphere imposes several limitations on the achievable performance levels. In this context, turbulence-induced scintillation (or fading) constitutes a critical impairment that severely degrades the performance of FSO links.

In order to combat fading and maintain acceptable performance levels, several fading mitigation techniques were proposed for FSO transmissions. These include collocated fading mitigation techniques where multiple apertures are deployed at the transmitter and/or receiver [2]–[5]. The second type of fading mitigation techniques corresponds to the distributed solutions which are based on user cooperation where neighboring nodes serve as relays between a source node and a destination node [6]–[17]. These recent relay-assisted FSO solutions that are attracting an increased research effort were inspired from the well known cooperative Radio-Frequency (RF) systems that were extensively investigated for more than a decade [18]. In the context of relay-assisted FSO communications, amplify-and-forward (AF) relaying was studied in [6], [7] and the solutions in [6], [8]–[15] were based on decode-and-forward (DF) cooperation. While the solutions in [6]–[12] are based on activating all available relays, a relay selection approach was adopted in [13] where a single relay is selected to participate in the cooperation effort. The performance of selective relaying and the corresponding reductions in the fading variance were derived in [14]. Within the same context, it was proven in [15] that under the quantum-limit scenario the optimal strategy consists of transmitting all data either along the direct link or along one of the indirect links via one relay that is appropriately chosen among all available relays. The implementation of the relay selection protocols in [13]–[15] necessitates acquiring the CSI of the underlying links.

On the other hand, none of the existing relay-assisted FSO systems exploited the potential existence of FSO links interconnecting the relays. For example, the parallel-relaying schemes in [6]–[15] are based on a two-phase strategy where a signal is transmitted from S to the relays in the first phase and then forwarded from these relays to D in the second phase. In this paper, we analyze for the first time cooperative FSO networks in the presence of inter-relay connections. As in parallel-relaying, a signal is first transmitted from S to the relays; however, instead of directly forwarding the processed signals to D, the relays cooperate with each other to enhance the fidelity of the corresponding reconstructed signals before forwarding these signals to D. This can be better illustrated in Fig. 1 that shows a typical FSO Metropolitan Area Network (MAN). It is assumed that the transceivers on buildings (2) and (3) are available for cooperation in order to enhance the communication reliability between buildings (1) and (4). Relabeling buildings (1), (2), (3) and (4), these will be referred to as S, R_1, R_2 and D, respectively. Note how, given the non-broadcast nature of FSO transmissions, one couple of FSO transceiver units is dedicated for each link. In previous contributions [6]–[17], the influence of the potential presence of a FSO link between buildings (2) and (3) was not studied. In our work, the possible presence of links of this kind was exploited for further boosting the performance of cooperative FSO networks. Note that the FSO connection between buildings (2) and (3) is not established for the purpose of realizing inter-relay cooperation; however, it is established initially to allow the exchange of information between buildings (2) and (3). If this additional resource is shared in the context of collaborative communications, our paper studies the effect of this additional degree of freedom on the system performance.

At a first time, we derive the expressions for the conditional error probability of the proposed scheme in the presence

The authors are with the Department of Electrical and Computer Engineering of the Lebanese American University (LAU), Byblos, Lebanon. (e-mails: {chadi.abourjeily,serj.haddad}@lau.edu.lb).

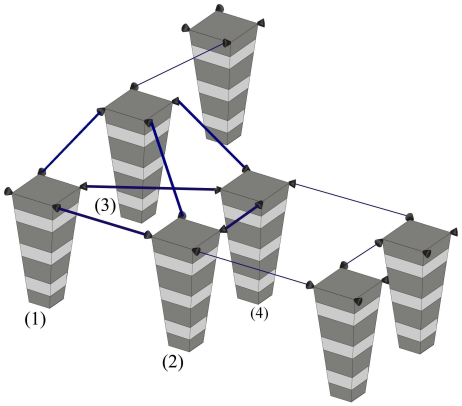

Fig. 1. An example of a mesh FSO network. Cooperation is proposed among the transceivers on buildings (1), (2), (3) and (4).

of background radiation with any number of relays and for any distribution of the available transmit power among the FSO links. Our second contribution consists of proposing an adapted power allocation strategy (PAS) that is crucial for the usefulness of the cooperation scheme in order to avoid spreading out the power inefficiently among the numerous links. In fact, for a N-relay network, the number of links increases from $2N{+}1$ in the absence of inter-relay connections (1 S-D, N S-R and N R-D links) to $3N$ in the presence of inter-relay connections ($N-1$ R-R links are added) as shown in Fig. 3 for $N = 3$. The proposed PAS is based on analytically minimizing the asymptotic conditional error probability in the case of negligible background radiation. The minimization is performed by applying the method of Lagrange multipliers with the solution satisfying the Karush-Kuhn-Tucker (KKT) conditions [19] for ensuring non-negative powers. In this context, we are adopting the classical approach of designing fading mitigation techniques and PASs for asymptotic signal-to-noise ratios where the expressions of the error probability are simpler and lend themselves to a simple analytical evaluation. The adopted approach results in a closed-form PAS that can be easily implemented in realistic FSO systems where the deployment of numerical optimization algorithms at the communicating nodes is infeasible from a practical point of view.

The rest of the paper is organized as follows. In section II, the main system parameters and the proposed cooperation strategy are described. The performance of the proposed scheme and the PAS are derived in section III first for two-relay systems followed by N-relay systems. Numerical results over gamma-gamma fading channels are provided in section IV while section V concludes the paper.

II. System Model and Cooperation Strategy

Consider the case where N relays are present in the geographical vicinity of a source node S and a destination node D where we assume the presence of a direct link between S and D. The relays will be denoted by R_1, ..., R_N in what follows. Each relay is connected to both S and D and, contrary to the existing literature, we also assume that any two consecutive relays R_n and R_{n+1} are interconnected. For the sake of unifying the notation, S and D will be denoted by R_0 and R_{N+1}.

The turbulence-induced fading gain (irradiance) between nodes R_m and R_n is dented by $I_{m,n}$. In this work, we adopt the gamma-gamma fading model [10]–[13] where the probability density function of the irradiance $I > 0$ is given by:

$$f(I) = \frac{2(\alpha\beta)^{(\alpha+\beta)/2}}{\Gamma(\alpha)\Gamma(\beta)} I^{(\alpha+\beta)/2-1} K_{\alpha-\beta}\left(2\sqrt{\alpha\beta I}\right) \quad (1)$$

where $\Gamma(.)$ is the Gamma function and $K_c(.)$ is the modified Bessel function of the second kind of order c. For a link distance d, the parameters α and β can be written as:

$$\alpha(d) = \left[\exp\left(0.49\sigma_R^2(d)/(1+1.11\sigma_R^{12/5}(d))^{7/6}\right) - 1\right]^{-1} \quad (2)$$

$$\beta(d) = \left[\exp\left(0.51\sigma_R^2(d)/(1+0.69\sigma_R^{12/5}(d))^{5/6}\right) - 1\right]^{-1} \quad (3)$$

where $\sigma_R^2(d)$ is the Rytov variance:

$$\sigma_R^2(d) = 1.23 C_n^2 k^{7/6} d^{11/6} \quad (4)$$

where k is the wave number and C_n^2 denotes the refractive index structure parameter.

Consider Q-ary pulse position modulation (PPM) with intensity-modulation and direct-detection (IM/DD). The average number of photoelectrons generated by the incident light signal in a PPM slot is given by [2]:

$$\lambda_s = \eta \frac{P_r T_s/Q}{hc/\lambda} = \eta \frac{E_s}{hc/\lambda} \quad (5)$$

where T_s is the symbol duration, h is Planck's constant, c is the speed of light, $\lambda = 1550$ nm is the wavelength and $\eta = 0.5$ is the detector's quantum efficiency. P_r stands for the optical signal power that is incident on the receiver and $E_s = P_r T_s/Q$ corresponds to the received optical energy per PPM slot along the direct link S-D. Based on the above notations, the average number of photoelectrons generated by background radiation (and dark currents) in a PPM slot is given by [2]:

$$\lambda_b = \eta \frac{P_b T_s/Q}{hc/\lambda} = \eta \frac{E_b}{hc/\lambda} \quad (6)$$

where P_b is the power of background noise and E_b stands for the energy of noise per PPM slot.

Transmissions occur in frames (or packets) each comprising a number of information and redundant symbols and occupying a time interval that will be referred to as a slot. Error-detecting codes are implemented and a cyclic redundancy check (CRC) is performed at each receiving node to determine whether the corresponding frame is correctly detected or not. We denote by $\mathbf{f}_{m,n}$ the frame transmitted from R_m to R_n. The notation $C_{m,n} = 1$ (resp. 0) means that the CRC evaluated at R_n corresponding to the frame transmitted from R_m is valid (resp. not valid) implying that the frame $\mathbf{f}_{m,n}$ was correctly (resp. erroneously) decoded. Finally, the relation $\mathbf{f}_{m,n} = \mathbf{0}$ indicates the absence of transmissions along the link $\mathrm{R}_m \rightarrow \mathrm{R}_n$.

The proposed cooperation strategy is realized over $2N$ time slots divided into four phases of transmission as follows.

Link	Slot #1	Slot #2	Slot #3	Slot #4	Slot #5	Slot #6
S→D	C.0					
S→R1	C.1					
S→R2	C.2					
S→R3	C.3					
R1→R2		C.4				
R2→R3			C.5			
R3→R2				C.6		
R2→R1					C.7	
R1→D						C.8
R2→D						C.9
R3→D						C.10

Fig. 2. Cooperation protocol with $N = 3$ relays.

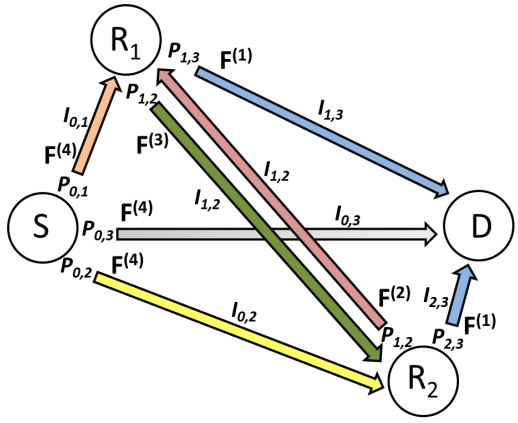

Fig. 3. Two-relay FSO network with interconnected relays.

Phase-I, S-D and S-R transmissions extending over one slot. In this phase, the links $\{\text{S}\rightarrow\text{D},\text{S}\rightarrow\text{R}_1,\ldots,\text{S}\rightarrow\text{R}_N\}$ are simultaneously activated where a frame $\mathbf{F}$ (to be communicated to D) is transmitted from S to D and to the relays in slot $n = 0$.

Phase-II, forward inter-relay (R-R) transmissions extending over $N - 1$ slots. In this phase, the links $\text{R}_1\rightarrow\text{R}_2,\ldots,\text{R}_{N-1}\rightarrow\text{R}_N$ are sequentially activated:

$$\mathbf{f}_{n,n+1}=\begin{cases}\mathbf{F}, & (C_{0,n}=1) \text{ or } (C_{n-1,n}=1\ ,\ n\neq 1);\\ \mathbf{0}, & \text{otherwise.}\end{cases} \quad (7)$$

In other words, transmissions are initiated along the link $\text{R}_n\rightarrow\text{R}_{n+1}$ under the condition that R_n has correctly acquired the frame $\mathbf{F}$. Note that, at this level, $\mathbf{F}$ could have been acquired either from S in slot 0 or from the previous relay R_{n-1} (if any) in slot $n-1$ (in the case where $n \neq 1$). In other words, if a valid CRC is attained along one of the links $\text{S}\rightarrow\text{R}_n$ or $\text{R}_{n-1}\rightarrow\text{R}_n$ (or both), then R_n retransmits the frame $\mathbf{F}$ that has been correctly decoded to the next relay R_{n+1}; otherwise, R_n switches off in the n-th slot.

Phase-III, backward inter-relay (R-R) transmissions extending over $N - 1$ slots. In this phase, the links $\text{R}_N\rightarrow\text{R}_{N-1},\ldots,\text{R}_2\rightarrow\text{R}_1$ are sequentially activated:

$$\mathbf{f}_{n,n-1}=$$
$$\begin{cases}\mathbf{F}, & [\mathbf{f}_{n-1,n}=\mathbf{0}]\ \&\ [(C_{0,n}=1) \text{ or } (C_{n+1,n}=1\ ,\ n\neq N)];\\ \mathbf{0}, & \text{otherwise.}\end{cases} \quad (8)$$

In other words, two conditions need to be satisfied for initiating backward transmissions along the link $\text{R}_n\rightarrow\text{R}_{n-1}$. (i): No frame was transmitted from R_{n-1} to R_n in phase-II ($\mathbf{f}_{n-1,n} = \mathbf{0}$) which shows (from (7)) that R_{n-1} did not acquire $\mathbf{F}$ justifying the interest of backward transmissions. Note that when $\mathbf{f}_{n-1,n} \neq \mathbf{0}$, $C_{n-1,n}$ might be equal to 0 or 1; but both cases indicate that transmissions occurred from R_{n-1} along $\text{R}_{n-1}\rightarrow\text{R}_n$ implying that R_{n-1} has acquired the value of $\mathbf{F}$ and there is no need to retransmit this frame along the link $\text{R}_n\rightarrow\text{R}_{n-1}$. (ii): R_n has acquired the value of $\mathbf{F}$ where, in this case, $\mathbf{F}$ could have been acquired either from S in slot 0 ($C_{0,n} = 1$) or from the next relay (if any) R_{n+1} ($C_{n+1,n} = 1$ for $n \neq N$).

Phase-IV, R-D transmissions extending over one slot. In the last slot, the relays that acquired $\mathbf{F}$ (either from S or from the subsequent and previous relays) forward the decoded frame to D by simultaneously activating the links $\{\text{R}_1\rightarrow\text{D},\ldots,\text{R}_N\rightarrow\text{D}\}$. $N + 1$ decision signals are available at D corresponding to the N frames $\mathbf{f}_{1,N+1},\ldots,\mathbf{f}_{N,N+1} \in \{\mathbf{0},\mathbf{F}\}$ transmitted by the relays and the frame $\mathbf{f}_{0,N+1} = \mathbf{F}$ transmitted by S. The destination decides in favor of any frame having a valid CRC.

The proposed cooperation protocol is better illustrated in Fig. 2 in the case of $N = 3$ relays. The conditions for activating the communications C.0-C.10 are as follows. Phase-I: C.0-C.3 are always activated. Phase-II: C.4 is activated if R_1 was able to acquire the frame $\mathbf{F}$ from S (through C.1); C.5 is activated if R_2 was able to acquire $\mathbf{F}$ from either S (through C.2) or R_1 (through C.4). Phase-III: C.6 is activated if R_3 did not receive anything from R_2 (through C.5) and R_3 was able to acquire $\mathbf{F}$ from S (through C.3); C.7 is activated if R_2 did not receive anything from R_1 (through C.4) and R_2 was able to acquire $\mathbf{F}$ from either S (through C.2) or R_3 (through C.6). Phase-IV: C.8 is activated if R_1 was able to acquire $\mathbf{F}$ from either S (through C.1) or R_2 (through C.7); C.9 is activated if R_2 was able to acquire $\mathbf{F}$ from S, R_1 or R_3 (through C.2, C.4 or C.6, respectively); C.10 is activated if R_3 was able to acquire $\mathbf{F}$ from either S (through C.3) or R_2 (through C.5).

Note that since the different transmissions are occurring over parallel non-interfering channels, then the proposed scheme does not suffer from any data-rate reduction compared to non-cooperative systems. In fact, after phase-I, the transmission of a new frame can be initiated from S to D and the relays. For example, for communicating the frames $\mathbf{F}^{(1)},\mathbf{F}^{(2)},\ldots$, Fig. 3 shows the state of a two-relay network during the fourth slot. Overall, the proposed scheme results simply in a decoding delay of $2N - 1$ slots. For example, in Fig. 2 with three relays, the decoding of the first frame takes place at slot 6.

Finally, note that while the proposed protocol can be associated with any PAS (in particular with uniform power allocation), we will prove in the following section that the optimal asymptotic PAS corresponds to activating a unique path between S and D which significantly simplifies the practical implementation of the proposed solution compared to the above $2N$-slot scheme.

III. Performance Analysis and Power Allocation

The proposed cooperation strategy ensures that the inter-relay communication occurs only in one direction, that is along either $R_n \rightarrow R_{n+1}$ (phase-II) or $R_{n+1} \rightarrow R_n$ (phase-III). In both cases, the fraction of the total power dedicated for this communication will be denoted by $P_{n,n+1}$. In the same way, we denote by $P_{0,n}$ and $P_{m,N+1}$ the fractions of the power allocated to links S-R_n and R_m-D for $n = 1, \ldots, N+1$ and $m = 1, \ldots, N$, respectively. Transmitting the same power as non-cooperative systems implies that:

$$\sum_{n=1}^{N+1} P_{0,n} + \sum_{n=1}^{N} P_{n,N+1} + \sum_{n=1}^{N-1} P_{n,n+1} = 1 \tag{9}$$

where the previous contributions in the literature follow as special cases by setting $P_{n,n+1} = 0$ for $n = 1, \ldots, N-1$, for example [15]. Note that in the proposed cooperation scheme (as in the case of serial and parallel relaying), a number of relays might remain idle; however, this effect can not be included in the power normalization. In fact, even when the distances and path gains between the nodes are known, it is impossible to predict which nodes will be idle since this depends on the specific realization of noise (that impacts the CRC's). Therefore, the power normalization in (9) corresponds to the worst case scenario (in terms of power consumption) in the sense that all links that can be active are effectively active. Similar approaches were adopted in [6], [13], for example.

The proposed PAS is based on minimizing the asymptotic conditional Frame Error Probability (FEP) where a frame is declared incorrect if at least one of its symbols is erroneous. Denote by $\mathbf{p}_{m,n}$ the probability that a nonzero frame transmitted by node m results in an invalid CRC at node n. From [14], this probability can be approximated by:

$$\mathbf{p}_{m,n} = \Pr\left(C_{m,n} = 0 \mid \mathbf{f}_{m,n} \neq \mathbf{0}\right) \tag{10}$$

$$\approx e^{-\left(\sqrt{g_c G_{m,n} I_{m,n} P_{m,n} \lambda_s + \lambda_b} - \sqrt{\lambda_b}\right)^2} = e^{-\gamma_{m,n}} \tag{11}$$

where the Chernoff bound was applied, as in [20], and where the above expression becomes very close to the exact error probability for large values of λ_s/λ_b. The coding gain g_c depends on the structure of the frames and is roughly equal to the rate of the implemented error-detecting code multiplied by its minimum distance for hard decision detection [21].

From (11), the term $\gamma_{m,n}$ is defined as:

$$\gamma_{m,n} = \left(\sqrt{g_c G_{m,n} I_{m,n} P_{m,n} \lambda_s + \lambda_b} - \sqrt{\lambda_b}\right)^2 \tag{12}$$

where $G_{m,n}$ is a gain factor associated with the link R_m-R_n that might be shorter than the direct link S-D. In this case, $G_{0,N+1} = 1$ and from [6]:

$$G_{m,n} = \left(\frac{d_{0,N+1}}{d_{m,n}}\right)^2 e^{-\sigma(d_{m,n} - d_{0,N+1})} \tag{13}$$

where σ is the attenuation coefficient and $d_{m,n}$ is the distance between R_m and R_n.

Equations (11) and (12) constitute the basis of the subsequent analysis that can be applied with any coding scheme. Note that (12) depends primarily on the irradiance $I_{m,n}$ while all other quantities are just constants. For simplicity of notation, we define:

$$k_{m,n} \triangleq g_c G_{m,n} I_{m,n} \lambda_s \tag{14}$$

where $\gamma_{m,n} \rightarrow P_{m,n} k_{m,n}$ for $\lambda_b \ll \lambda_s$; that is, when the power of background noise is negligible compared to the signal power.

Note that $G_{m,n} = G_{n,m}$ from (13). On the other hand, we assume that $I_{m,n} = I_{n,m}$ following from the reciprocity of the optical channel [22]. From (14), this implies that $k_{m,n} = k_{n,m}$ for all values of m and n. In the same way, $\gamma_{m,n} = \gamma_{n,m}$.

The PAS is first derived for a 2-relay system and will be further extended to a N-relay system.

A. Two Relays

Since a correct decision is guaranteed at D when a valid CRC is attained along the direct link S-D, the conditional FEP can be written as:

$$\begin{aligned} P_e = \mathbf{p}_{0,3} \big[&\mathbf{p}_{1,3}\mathbf{p}_{2,3} q_1 + (1 - \mathbf{p}_{1,3})\mathbf{p}_{2,3} q_2 \\ &+ \mathbf{p}_{1,3}(1 - \mathbf{p}_{2,3}) q_3 + (1 - \mathbf{p}_{1,3})(1 - \mathbf{p}_{2,3}) q_4\big] \end{aligned} \tag{15}$$

where $q_1, \ldots, q_4$ stand for the error probabilities under different states of the R-D links. Evidently, $q_1 = 1$ since in this case whether any of the relays R_1 and R_2 is switched off or transmitting a nonzero frame, the corresponding CRC at D will be invalid. For evaluating q_2, the CRC corresponding to the link $R_2 \rightarrow$D can not be valid following from either the switching off of R_2 or from the impairments along the link $R_2 \rightarrow$D. In this case, the decision at D will be based on the signal it receives from R_1. If R_1 is switched off an error will occur at D; otherwise, the nonzero frame transmitted by R_1 will result in a correct decision at D. Consequently, q_2 corresponds to the probability that R_1 is switching off. Now, R_1 switches off when it receives invalid CRCs via the parallel paths S$\rightarrow R_1$ and S$\rightarrow R_2 \rightarrow R_1$:

$$\begin{aligned} q_2 &= \mathbf{p}_{0,1}\left[1 - (1 - \mathbf{p}_{0,2})(1 - \mathbf{p}_{2,1})\right] \\ &= e^{-\gamma_{0,1}}\left[e^{-\gamma_{0,2}} + e^{-\gamma_{2,1}} - e^{-\gamma_{0,2}} e^{-\gamma_{2,1}}\right] \end{aligned} \tag{16}$$

In the same way, $q_3 = e^{-\gamma_{0,2}}\left[e^{-\gamma_{0,1}} + e^{-\gamma_{1,2}} - e^{-\gamma_{0,1}} e^{-\gamma_{1,2}}\right]$. For evaluating q_4, a nonzero frame transmitted from either R_1 or R_2 will result in a correct decision at D. In other words, no valid CRC will be observed at D only if both R_1 and R_2 are switching off which in turn can occur only because of the simultaneous failure of the S-R_1 and S-R_2 links irrespective of the state of the R_1-R_2 link: $q_4 = \mathbf{p}_{0,1}\mathbf{p}_{0,2} = e^{-\gamma_{0,1}} e^{-\gamma_{0,2}}$. Replacing the corresponding probabilities in (15) results in:

$$\begin{aligned} P_e = e^{-\gamma_{0,3}} \big[&e^{-\gamma_{1,2}}\left(e^{-\gamma_{0,1}} + e^{-\gamma_{1,3}} - e^{-\gamma_{0,1}} e^{-\gamma_{1,3}}\right) \\ &\left(e^{-\gamma_{0,2}} + e^{-\gamma_{2,3}} - e^{-\gamma_{0,2}} e^{-\gamma_{2,3}}\right) + \left(1 - e^{-\gamma_{1,2}}\right) \\ &\left(e^{-\gamma_{0,1}} e^{-\gamma_{0,2}} + e^{-\gamma_{1,3}} e^{-\gamma_{2,3}} - e^{-\gamma_{0,1}} e^{-\gamma_{0,2}} e^{-\gamma_{1,3}} e^{-\gamma_{2,3}}\right)\big] \end{aligned} \tag{17}$$

The last expression does not lend itself to an analytical minimization and, consequently, we will resort to an asymptotic analysis for deriving the PAS. Following from the rapid exponential decay of the probability in (11), the terms that

$$\mathbf{P}=\begin{cases}[1,0,0,0,0,0], & i=1;\\ [0,0,f_1(k_{0,1},k_{1,3}),f_2(k_{0,1},k_{1,3}),0,0]\,, & i=2;\\ [0,0,0,0,f_1(k_{0,2},k_{2,3}),f_2(k_{0,2},k_{2,3})]\,, & i=3;\\ [0,f_2(k_{0,1},k_{1,2},k_{2,3}),f_1(k_{0,1},k_{1,2},k_{2,3}),f_3(k_{0,1},k_{1,2},k_{2,3}),0,0]\,, & i=4;\\ [0,f_2(k_{0,2},k_{2,1},k_{1,3}),0,0,f_1(k_{0,2},k_{2,1},k_{1,3}),f_2(k_{0,2},k_{2,1},k_{1,3})]\,, & i=5.\end{cases} \quad (21)$$

correspond to the product of more than three exponentials in $e^{\gamma_{0,3}}P_e$ can be safely neglected. Replacing $\gamma_{m,n}$ by $P_{m,n}k_{m,n}$, (17) tends to the following asymptotic value:

$$P_e \doteq e^{-k_{0,3}P_{0,3}}\left[e^{-k_{0,1}P_{0,1}}e^{-k_{0,2}P_{0,2}}+e^{-k_{1,3}P_{1,3}}e^{-k_{2,3}P_{2,3}}\right.$$
$$\left.+e^{-k_{1,2}P_{1,2}}\left(e^{-k_{0,1}P_{0,1}}e^{-k_{2,3}P_{2,3}}+e^{-k_{0,2}P_{0,2}}e^{-k_{1,3}P_{1,3}}\right)\right] \quad (18)$$

where $x \doteq y$ means that x and y are asymptotically equal. In what follows, we define the vector $\mathbf{P}$ as: $\mathbf{P} = [P_{0,3}, P_{1,2}, P_{0,1}, P_{1,3}, P_{0,2}, P_{2,3}]$.

Proposition 1: For negligible background noise levels, the vector $\mathbf{P}$ that minimizes the asymptotic expression in (18) subject to (9) can be obtained as follows. Construct the set $\mathcal{I}$ as follows:

$$\mathcal{I}=\left\{\frac{1}{k_{0,3}},\frac{1}{k_{0,1}}+\frac{1}{k_{1,3}},\frac{1}{k_{0,2}}+\frac{1}{k_{2,3}},\right.$$
$$\left.\frac{1}{k_{0,1}}+\frac{1}{k_{1,2}}+\frac{1}{k_{2,3}},\frac{1}{k_{0,2}}+\frac{1}{k_{2,1}}+\frac{1}{k_{1,3}}\right\} \quad (19)$$

and define the integer i as:

$$i=\arg\min[\mathcal{I}] \quad (20)$$

The optimal solution is given in (21) shown at the top of the page where the functions $f_i(.)$ are defined as:

$$f_i(c_1,\ldots,c_n)=\frac{1}{c_i}\frac{1+\sum_{j=1}^{n}\frac{1}{c_j}\ln\left(\frac{c_i}{c_j}\right)}{\sum_{j=1}^{n}\frac{1}{c_j}} \quad ; \quad i=1,\ldots,n \quad (22)$$

Proof: The proof is provided in Appendix A. The constrained minimization is based on the method of Lagrange multipliers with the solution satisfying the Karush-Kuhn-Tucker (KKT) conditions [19] to ensure non-negative powers.

The performed minimization shows that the optimal solution corresponds to activating only one path among the paths S-D, S-R_1-D, S-R_2-D, S-R_1-R_2-D and S-R_2-R_1-D. The selection of the best path is based on (19)-(20) while the distribution of the power among the corresponding hops is determined by (21)-(22). An element of $\mathcal{I}$ quantifies the inverse of the strength of the corresponding path from S to D and (20) is equivalent to selecting the path with the maximum strength. Note that the solution obtained in [15] follows as a special case by setting $k_{1,2}=k_{2,1}=0$. In this case, the fourth and fifth elements of $\mathcal{I}$ in (19) will tend to infinity and, hence, will never satisfy (20).

B. N Relays

We next evaluate the conditional FEP with N relays. Consider the case where N_c "cuts" occur among the $N-1$ links interconnecting the relays and denote the indices of these cuts by $i_1,\ldots,i_{N_c}$. These cuts correspond to the erroneous detection of the nonzero frames transmitted along the N_c links R_{i_1}-R_{i_1+1}, …, $R_{i_{N_c}}$-$R_{i_{N_c}+1}$ while realizing correct decisions along the remaining $N-1-N_c$ links interconnecting two consecutive relays. The probability of occurrence of this scenario can be written as:

$$\prod_{j\in\{i_1,\ldots,i_{N_c}\}}e^{-\gamma_{j,j+1}}\prod_{j\in\{1,\ldots,N-1\}\setminus\{i_1,\ldots,i_{N_c}\}}\left(1-e^{-\gamma_{j,j+1}}\right) \quad (23)$$

Under the above scenario, the N relays can be partitioned into the following clusters $\{1,\ldots,i_1\}$, $\{i_1+1,\ldots,i_2\}$, …, $\{i_{N_c}+1,\ldots,N\}$ where the relays in each cluster are interconnected (owing to valid CRCs if the relays are not switched off or, equivalently, correct detection of nonzero frames along the corresponding links). A given cluster ensures forwarding the frame $\mathbf{F}$ from S to D in all cases except when all links from S to this cluster fail simultaneously or when all links from the cluster to D fail simultaneously. In other words, the probability of not observing any valid CRC at D via the cluster $\{i_{k-1}+1,\ldots,i_k\}$ can be written as:

$$=\prod_{j=i_{k-1}+1}^{i_k}e^{-\gamma_{0,j}}+\prod_{j=i_{k-1}+1}^{i_k}e^{-\gamma_{j,N+1}}-\prod_{j=i_{k-1}+1}^{i_k}e^{-\gamma_{0,j}}e^{-\gamma_{j,N+1}} \quad (24)$$

where $i_0 \triangleq 0$ and $i_{N_c+1} \triangleq N$.

Finally, combining (23) and (24) results in:

$$P_e = e^{-\gamma_{0,N+1}}\sum_{N_c=0}^{N-1}\sum_{(i_1,\ldots,i_{N_c})\in\mathcal{I}_1^{(N_c)}\ldots\mathcal{I}_{\binom{N-1}{N_c}}^{(N_c)}}$$
$$\prod_{j\in\{i_1,\ldots,i_{N_c}\}}e^{-\gamma_{j,j+1}}\prod_{j\in\{1,\ldots,N-1\}\setminus\{i_1,\ldots,i_{N_c}\}}\left(1-e^{-\gamma_{j,j+1}}\right)\prod_{k=1}^{N_c+1}$$
$$\left[\prod_{j=i_{k-1}+1}^{i_k}e^{-\gamma_{0,j}}+\prod_{j=i_{k-1}+1}^{i_k}e^{-\gamma_{j,N+1}}-\prod_{j=i_{k-1}+1}^{i_k}e^{-\gamma_{0,j}}e^{-\gamma_{j,N+1}}\right] \quad (25)$$

where $\mathcal{I}_1^{(N_c)},\ldots,\mathcal{I}_{\binom{N-1}{N_c}}^{(N_c)}$ are all possible subsets of $\{1,\ldots,N-1\}$ having N_c elements each.

We next resort to upper-bounding (25) so that an analytical solution of the power allocation can be obtained from this simple bound. The approach for upper-bounding (25) is to ignore all terms in $e^{\gamma_{0,N+1}}P_e$ corresponding to the product of more than $N+1$ decreasing exponential functions. Note that $e^{\gamma_{0,N+1}}P_e$ contains terms that correspond to the product of N and $N+1$ exponential functions and the bound is based on keeping only these terms. For example, for $N=2$, the bound in (18) on $e^{\gamma_{0,3}}P_e$ keeps only the terms corresponding to the product of 2 and 3 exponential functions.

Since all the relays are partitioned over the different clusters, the last term in (25) ($\prod_{k=1}^{N_c+1}[\cdots]$) corresponds to the summation of different terms consisting of the product of N

$$e^{\gamma_{0,N+1}}P_e^{(N_c=1)} = \sum_{i=1}^{N-1} e^{-\gamma_{i,i+1}} \prod_{j=1\ ;\ j\neq i}^{N-1} \left(1-e^{-\gamma_{j,j+1}}\right) \left[\prod_{j=1}^{i} e^{-\gamma_{0,j}} + \prod_{j=1}^{i} e^{-\gamma_{j,N+1}} - \prod_{j=1}^{i} e^{-\gamma_{0,j}} e^{-\gamma_{j,N+1}}\right] \left[\prod_{j=i+1}^{N} e^{-\gamma_{0,j}} + \prod_{j=i+1}^{N} e^{-\gamma_{j,N+1}} - \prod_{j=i+1}^{N} e^{-\gamma_{0,j}} e^{-\gamma_{j,N+1}}\right]$$
$$\doteq \sum_{i=1}^{N-1} e^{-\gamma_{i,i+1}} \left[\prod_{j=1}^{N} e^{-\gamma_{0,j}} + \prod_{j=1}^{N} e^{-\gamma_{j,N+1}} + \prod_{j=1}^{i} e^{-\gamma_{0,j}} \prod_{j=i+1}^{N} e^{-\gamma_{j,N+1}} + \prod_{j=1}^{i} e^{-\gamma_{j,N+1}} \prod_{j=i+1}^{N} e^{-\gamma_{0,j}}\right] \quad (27)$$

or more exponential functions. In the same way, the term $\prod_j e^{-\gamma_{j,j+1}}$ corresponds to the product of N_c exponential functions while the term $\prod_j(1-e^{-\gamma_{j,j+1}})$ is composed of terms corresponding to the product of 0 or more exponential functions. Consequently, for obtaining the upper-bound, N_c is restricted to either 0 or 1 in (25). For $N_c=0$, the corresponding term in (25) can be written as:

$$e^{\gamma_{0,N+1}}P_e^{(N_c=0)} = \prod_{j=1}^{N-1}\left(1-e^{-\gamma_{j,j+1}}\right) \left[\prod_{j=1}^{N} e^{-\gamma_{0,j}} + \prod_{j=1}^{N} e^{-\gamma_{j,N+1}} - \prod_{j=1}^{N} e^{-\gamma_{0,j}} e^{-\gamma_{j,N+1}}\right]$$
$$\doteq \left(1-\sum_{j=1}^{N-1} e^{-\gamma_{j,j+1}}\right)\left[\prod_{j=1}^{N} e^{-\gamma_{0,j}} + \prod_{j=1}^{N} e^{-\gamma_{j,N+1}}\right] \quad (26)$$

For $N_c=1$, the corresponding term in (25) can be written as shown in (27) at the top of the page (where $i \triangleq i_1$). Finally, combining (26) and (27) and replacing $\gamma_{m,n}$ by $P_{m,n}k_{m,n}$ for large signal-to-noise ratios results in (28) shown at the bottom of the page.

Proposition 2: For negligible background noise levels, the PAS that minimizes the asymptotic expression in (28) subject to (9) corresponds to selecting a unique path between S and D and distributing the power among its hops according to (22). The path with the minimum sum of inverse path gains (k's) is selected.

Proof: The proof is provided in Appendix B.

For example, consider the (N_h+2)-hop path S-$\mathrm{R}_n\rightarrow\mathrm{R}_{n+1}\rightarrow\cdots\rightarrow\mathrm{R}_{n+N_h}\rightarrow$D. The inverse-strength of this path is $\frac{1}{k_{0,n}}+\sum_{m=1}^{N_h}\frac{1}{k_{n+m-1,n+m}}+\frac{1}{k_{n+N_h,N+1}}$ where the path with the minimum inverse-strength (or maximum strength) is selected in analogy with (19) and (20) in the case of $N=2$. From (22), the power allocated to the i-th hop of this path is given by $f_i(k_{0,n}, k_{n,n+1}, \cdots, k_{n+N_h-1,n+N_h}, k_{n+N_h,N+1})$. Note that paths of the form S$\rightarrow\mathrm{R}_n\rightarrow\mathrm{R}_{n-1}\rightarrow\cdots\rightarrow\mathrm{R}_{n-N_h}\rightarrow$D can also be selected based on the proposed cooperation strategy. Overall, there are 1 one-hop path, N two-hop paths, $2(N-1)$ three-hop paths, $2(N-2)$ four-hop paths, ... resulting in a total of N^2+1 possible paths.

Note that the proposed PAS corresponds to an asymptotic solution that holds for negligible levels of background radiation. For scenarios where the power of background noise is high, the optimal solution might necessitate activating more than one path between the source and destination. Note also that the implementation of the proposed PAS requires the knowledge of the $3N$-dimensional vector $\mathbf{K} \triangleq [k_{0,N+1}, k_{0,1}, \ldots, k_{0,N}, k_{1,N+1}, \ldots, k_{N,N+1}, k_{1,2}, \ldots, k_{N-1,N}]$ and hence necessitates the estimation of the additional $N-1$ parameters $k_{1,2}, \ldots, k_{N-1,N}$ of the inter-relay links compared to parallel-relaying [15]. However, this additional complexity is associated with significant performance gains as will be highlighted in the next section. In this context, the proposed solution can take advantage from the large coherence times of the FSO channels. Note also that all elements of $\mathbf{K}$ are proportional to $g_c\lambda_s$ implying that the selection of the best path is independent from the signal strength. In other words, $k_{m,n}$ can be replaced by $G_{m,n}I_{m,n}$ in (19)-(20).

IV. Numerical Results

We set $C_n^2 = 1.7\times10^{-14}$ m$^{-2/3}$ and $\sigma = 0.43$ dB/km in (4) and (13), respectively. We show the simulation results for a FSO network characterized by the following geometrical parameters. (i): The distance between S and D is set to $d_{0,N+1} = 5$ km. (ii): The distances of the first relay from S and D are set to $d_{0,1} = 2$ km and $d_{1,N+1} = 4$ km, respectively. (iii): The N-th relay occupies a symmetrical position characterized by the following distances: $d_{0,N} = 4$ km and $d_{N,N+1} = 2$ km. (iv): The remaining $N-2$ relays are placed equidistantly between relays R_1 and R_N. Following from (5) and (14), the performance of the proposed system will

$$P_e \doteq e^{-k_{0,N+1}P_{0,N+1}}\left[\prod_{j=1}^{N} e^{-k_{0,j}P_{0,j}} + \prod_{j=1}^{N} e^{-k_{j,N+1}P_{j,N+1}} + \sum_{i=1}^{N-1} e^{-k_{i,i+1}P_{i,i+1}} \times \left(\prod_{j=1}^{i} e^{-k_{0,j}P_{0,j}} \prod_{j=i+1}^{N} e^{-k_{j,N+1}P_{j,N+1}} + \prod_{j=1}^{i} e^{-k_{j,N+1}P_{j,N+1}} \prod_{j=i+1}^{N} e^{-k_{0,j}P_{0,j}}\right)\right] \quad (28)$$

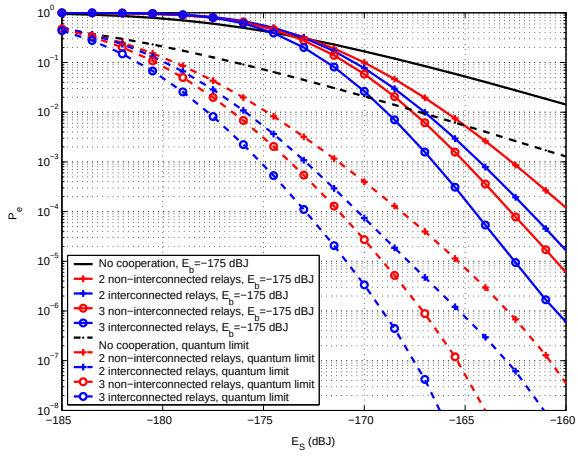

Fig. 4. Impact of the signal energy with all-active relaying.

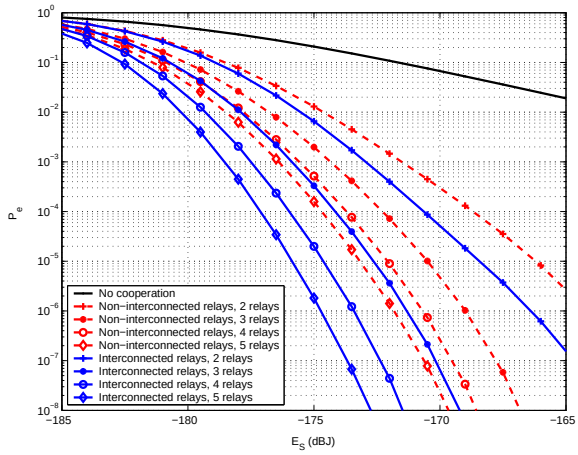

Fig. 5. Impact of the signal energy at $E_b = -185$ dBJ.

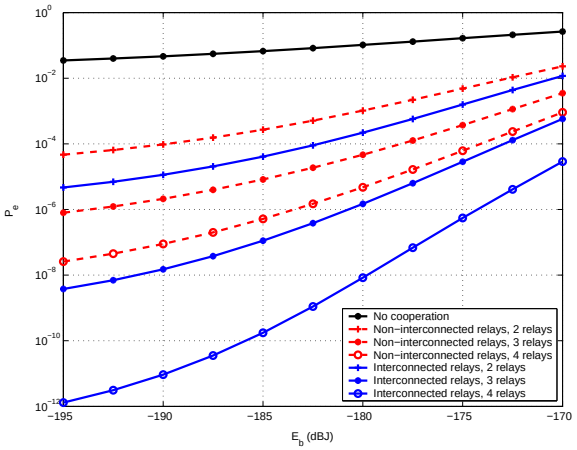

Fig. 6. Impact of the noise energy at $E_S = -170$ dBJ.

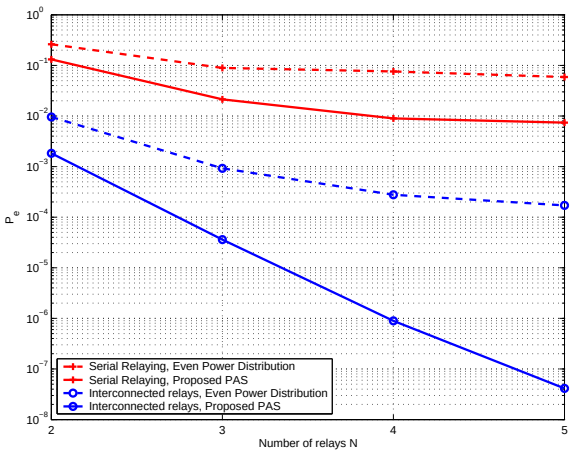

Fig. 7. The proposed scheme versus serial relaying at $E_S = -172$ dBJ and $E_b = -180$ dBJ.

be parameterized by $E_S \triangleq g_c E_s$. This approach is adopted for the sake of rendering the presented results independent from the structure of the implemented error-detecting code.

In Fig. 4 we compare the proposed cooperation strategy (with interconnected-relays) to the parallel-relaying strategy (with non interconnected-relays) in the case of all-active relaying with uniform power allocation. In other words, for non interconnected-relays the transmit power is evenly split among the $2N+1$ S-D, S-R and R-D links [6]. On the other hand, for interconnected-relays the transmit power is evenly split among the $3N$ S-D, S-R, R-D and R-R links. Fig. 4 shows the performance as a function of E_S for $E_b = -175$ dBJ as well as for the quantum limit with no background radiation (where the only source of noise is the shot noise). This figure shows that comparable performance trends are observed in the presence or absence of background noise. Moreover, results show the superiority of the proposed scheme despite the fact that the transmit power is spread over a larger number of links.

In the subsequent figures, the proposed PAS is applied resulting in further enhancements in the performance levels. A numerical analysis showed that the proposed PAS which is based on analytically minimizing the asymptotic expressions in (18) and (28) is extremely close to the strategy based on numerically minimizing the exact error probability expressions in (17) and (25). Under all simulation setups, the FEP curves corresponding to the above approaches were undistinguishable thus highlighting the interest of the proposed closed-from asymptotically-optimal solution.

In Fig. 5 and Fig. 6 we compare the proposed cooperation strategy with the parallel-relaying strategy in the case where an optimized PAS is applied. For the case of interconnected-relays the proposed PAS is applied while for non interconnected relays the PAS proposed in [15] is applied. Note that both our work and [15] apply a similar PAS in the sense of adequately spreading the transmit power among the hops of the strongest path connecting S to D. In particular, the solution in [15] follows as a special case of proposition 1 and proposition 2 by setting the inter-relay gains to zero. Fig. 5 shows the performance as a function of E_S for $E_b = -185$ dBJ. Results show the high performance levels that can be achieved in scenarios where inter-relay connections are available. For example, at $P_e = 10^{-4}$, the performance gains are 2 dB and 2.5 dB with $N = 2$ and $N = 5$, respectively. These gains follow from the possibility of transmitting along paths comprising more than two hops. For example, for $N = 3$ in

the absence of inter-relay connections, 1-hop and 2-hop links are selected around 16% and 84% of the time, respectively, while in the presence of inter-relay connections, 1-hop, 2-hop, 3-hop and 4-hop links are selected around 11%, 50%, 31% and 8% of the time, respectively. Fig. 6 investigates the impact of background radiation on the error performance at $E_S = -170$ dBJ. The enhancements resulting from the presence of inter-relay connections are evident for all values of E_b. Moreover, the performance gap between systems deploying inter-relay cooperation and those not deploying this solution increases with the number of relays. For example, with four interconnected relays, error rates as small as 10^{-12} can be achieved at $E_b = -195$ dBJ.

Fig. 7 compares the proposed cooperation scheme with serial relaying where all information messages are relayed along the $(N+1)$-hop shortest path S-R_1-$\cdots$-R_N-D at $E_S = -172$ dBJ and $E_b = -180$ dBJ. Serial relaying is associated with both the uniform power allocation strategy (as in [6]) as well as the proposed PAS. Moreover, in order to show the importance of distributing the available power among the hops according to (22), we investigate a simplified PAS that can be associated with the proposed cooperation scheme. This simplified PAS corresponds to evenly distributing the power among the hops once the strongest path is selected according to proposition 2. This approach avoids the estimation of E_S and the evaluation of the logarithmic function in (22). Results show the superiority of the proposed inter-relay cooperation scheme compared to serial relaying especially for large number of relays. The importance of implementing the proposed PAS is also highlighted in this figure. Note that despite the fact that the path S-R_1-$\cdots$-R_N-D comprises the shortest hops (having the smallest fading variances according to the adopted channel model), in the proposed asymptotically optimal solution, this path is selected only around 17.5%, 8%, 6% and 4.8% of the time for $N = 2$, 3, 4 and 5, respectively. Note that the other $(N+1)$-hop path S-R_N-$\cdots$-R_1-D is almost never selected following from the geometry of the network.

V. Conclusion

Despite the huge progress and high performance gains reported in the literature of relay-assisted FSO communications, further enhancements are still possible based on the concept of inter-relay cooperation; an idea introduced in this paper and that constitutes an important degree of freedom that has never been investigated before. Taking advantage of the presence of inter-relay connections can significantly boost the performance of cooperative FSO networks since the fading variance along a FSO link decreases with its distance. In particular, substantial improvements were observed over an aggregated channel model that takes into consideration both path-loss and turbulence-induced fading. The proposed solution that requires the knowledge of the CSI can take advantage from the large coherence time of FSO systems where the estimates of the underlying channels, and hence the transmitted powers, do not need to be updated very often. We hope that this work will trigger more research effort in this promising direction.

Appendix A
Power Allocation with Two Relays

Construct the set $\mathcal{S}$ as $\mathcal{S} = \{(0,3),(1,2),(0,1),(1,3),(0,2),(2,3)\}$. In order to minimize (18) subject to the equality constraint $\sum_{(m,n)\in\mathcal{S}} P_{m,n} = 1$ (which is equivalent to (9)) and the six inequality constraints $-P_{m,n} \leq 0$ for $(m,n) \in \mathcal{S}$, we construct the Lagrangian function:

$$\mathcal{L} = e^{-k_{0,3}P_{0,3}}\left[e^{-k_{0,1}P_{0,1}}e^{-k_{0,2}P_{0,2}} + e^{-k_{1,3}P_{1,3}}e^{-k_{2,3}P_{2,3}} + e^{-k_{1,2}P_{1,2}}\left(e^{-k_{0,1}P_{0,1}}e^{-k_{2,3}P_{2,3}} + e^{-k_{0,2}P_{0,2}}e^{-k_{1,3}P_{1,3}}\right)\right] + \lambda\left(\sum_{(m,n)\in\mathcal{S}} P_{m,n} - 1\right) - \sum_{(m,n)\in\mathcal{S}} \mu_{m,n}P_{m,n} \quad (29)$$

For the sake of notational simplicity, we define $\delta_{m,n} \triangleq k_{m,n}P_{m,n}$. At the optimal point $\mathbf{P}$, $\mathcal{L}$ must satisfy the following equations:

$$\frac{\partial\mathcal{L}}{\partial P_{0,3}} = -k_{0,3}e^{-\delta_{0,3}}\left[e^{-\delta_{0,1}}e^{-\delta_{0,2}} + e^{-\delta_{1,3}}e^{-\delta_{2,3}} + e^{-\delta_{1,2}}\left(e^{-\delta_{0,1}}e^{-\delta_{2,3}} + e^{-\delta_{0,2}}e^{-\delta_{1,3}}\right)\right] + \lambda - \mu_{0,3} = 0 \quad (30)$$

$$\frac{\partial\mathcal{L}}{\partial P_{0,1}} = -k_{0,1}e^{-\delta_{0,3}}e^{-\delta_{0,1}}\left[e^{-\delta_{0,2}} + e^{-\delta_{1,2}}e^{-\delta_{2,3}}\right] + \lambda - \mu_{0,1} = 0 \quad (31)$$

$$\frac{\partial\mathcal{L}}{\partial P_{0,2}} = -k_{0,2}e^{-\delta_{0,3}}e^{-\delta_{0,2}}\left[e^{-\delta_{0,1}} + e^{-\delta_{1,2}}e^{-\delta_{1,3}}\right] + \lambda - \mu_{0,2} = 0 \quad (32)$$

$$\frac{\partial\mathcal{L}}{\partial P_{1,3}} = -k_{1,3}e^{-\delta_{0,3}}e^{-\delta_{1,3}}\left[e^{-\delta_{2,3}} + e^{-\delta_{1,2}}e^{-\delta_{0,2}}\right] + \lambda - \mu_{1,3} = 0 \quad (33)$$

as well as the equations:

$$\frac{\partial\mathcal{L}}{\partial P_{2,3}} = -k_{2,3}e^{-\delta_{0,3}}e^{-\delta_{2,3}}\left[e^{-\delta_{1,3}} + e^{-\delta_{1,2}}e^{-\delta_{0,1}}\right] + \lambda - \mu_{2,3} = 0 \quad (34)$$

$$\frac{\partial\mathcal{L}}{\partial P_{1,2}} = -k_{1,2}e^{-\delta_{0,3}}e^{-\delta_{1,2}}\left[e^{-\delta_{0,1}}e^{-\delta_{2,3}} + e^{-\delta_{0,2}}e^{-\delta_{1,3}}\right] + \lambda - \mu_{1,2} = 0 \quad (35)$$

$$\frac{\partial\mathcal{L}}{\partial\lambda} = P_{0,3} + P_{1,2} + P_{0,1} + P_{1,3} + P_{0,2} + P_{2,3} - 1 = 0 \quad (36)$$

The KKT conditions are given by:

$$\mu_{m,n}P_{m,n} = 0 \quad ; \quad (m,n) \in \mathcal{S} \quad (37)$$

$$\mu_{m,n} \geq 0 \quad ; \quad (m,n) \in \mathcal{S} \quad (38)$$

If $P_{1,2} = 0$, the proposed cooperation strategy is equivalent to [15] where inter-relay cooperation is not considered. From [15], the optimal solution corresponds to selecting the path among S-D, S-R_1-D and S-R_2-D having the maximum strength where the inverse-strengths of these paths are given by $\frac{1}{k_{0,3}}$, $\frac{1}{k_{0,1}} + \frac{1}{k_{1,3}}$ and $\frac{1}{k_{0,2}} + \frac{1}{k_{2,3}}$ (the first three elements of $\mathcal{I}$ in (19)), respectively.

We next investigate the solutions for which $P_{1,2} \neq 0$.

Solution 1: $P_{0,1} \neq 0$, $P_{1,2} \neq 0$, $P_{2,3} \neq 0$ and the remaining components of $\mathbf{P}$ are zero. From (37), $\mu_{0,1} = \mu_{1,2} = \mu_{2,3} = 0$

and the corresponding inequalities in (38) are satisfied. Replacing these values in (31), (35) and (34) results in:

$$\lambda = k_{0,1}e^{-\delta_{0,1}}\left[1+e^{-\delta_{1,2}}e^{-\delta_{2,3}}\right] \doteq k_{0,1}e^{-\delta_{0,1}} \quad (39)$$

$$\lambda = k_{1,2}e^{-\delta_{1,2}}\left[e^{-\delta_{0,1}}e^{-\delta_{2,3}}+1\right] \doteq k_{1,2}e^{-\delta_{1,2}} \quad (40)$$

$$\lambda = k_{2,3}e^{-\delta_{2,3}}\left[1+e^{-\delta_{1,2}}e^{-\delta_{0,1}}\right] \doteq k_{2,3}e^{-\delta_{2,3}} \quad (41)$$

Solving the above equations in addition to (36) (that can be written as $P_{0,1}+P_{1,2}+P_{2,3}=1$) results in the solution given in (22).

Since $\mu_{0,3} \geq 0$ from (38), equation (30) can be written as:

$$\begin{aligned}\mu_{0,3} &= \lambda - k_{0,3}\left[e^{-\delta_{0,1}}+e^{-\delta_{2,3}}+e^{-\delta_{1,2}}\left(e^{-\delta_{0,1}}e^{-\delta_{2,3}}+1\right)\right] \\ &\doteq \lambda - k_{0,3}\left[e^{-\delta_{0,1}}+e^{-\delta_{2,3}}+e^{-\delta_{1,2}}\right] \\ &= \lambda - k_{0,3}\lambda\left[\frac{1}{k_{0,1}}+\frac{1}{k_{2,3}}+\frac{1}{k_{1,2}}\right] \geq 0 \end{aligned} \quad (42)$$

where (39)-(41) were invoked in (42). Finally, (42) implies that:

$$\frac{1}{k_{0,1}}+\frac{1}{k_{1,2}}+\frac{1}{k_{2,3}} \leq \frac{1}{k_{0,3}} \quad (43)$$

Since $\mu_{0,2} \geq 0$ from (38), equation (32) can be written as:

$$\mu_{0,2} = \lambda - k_{0,2}\left[e^{-\delta_{0,1}}+e^{-\delta_{1,2}}\right] = \lambda - k_{0,2}\lambda\left[\frac{1}{k_{0,1}}+\frac{1}{k_{1,2}}\right] \geq 0 \quad (44)$$

implying that $\frac{1}{k_{0,1}}+\frac{1}{k_{1,2}} \leq \frac{1}{k_{0,2}}$. Adding the term $\frac{1}{k_{2,3}}$ to both sides of this inequality results in:

$$\frac{1}{k_{0,1}}+\frac{1}{k_{1,2}}+\frac{1}{k_{2,3}} \leq \frac{1}{k_{0,2}}+\frac{1}{k_{2,3}} \quad (45)$$

Since $\mu_{1,3} \geq 0$ from (38), equation (33) can be written as:

$$\mu_{1,3} = \lambda - k_{1,3}\left[e^{-\delta_{2,3}}+e^{-\delta_{1,2}}\right] = \lambda - k_{1,3}\lambda\left[\frac{1}{k_{2,3}}+\frac{1}{k_{1,2}}\right] \geq 0 \quad (46)$$

implying that $\frac{1}{k_{1,2}}+\frac{1}{k_{2,3}} \leq \frac{1}{k_{1,3}}$. Adding the term $\frac{1}{k_{0,1}}$ to both sides of this inequality results in:

$$\frac{1}{k_{0,1}}+\frac{1}{k_{1,2}}+\frac{1}{k_{2,3}} \leq \frac{1}{k_{0,1}}+\frac{1}{k_{1,3}} \quad (47)$$

Finally, adding the inequalities $\frac{1}{k_{0,1}}+\frac{1}{k_{1,2}} \leq \frac{1}{k_{0,2}}$ and $\frac{1}{k_{1,2}}+\frac{1}{k_{2,3}} \leq \frac{1}{k_{1,3}}$ and adding the term $\frac{1}{k_{1,2}}$ to both sides of the obtained inequality results in $\frac{1}{k_{0,1}}+\frac{2}{k_{1,2}}+\frac{1}{k_{2,3}} \leq \frac{1}{k_{0,2}}+\frac{1}{k_{1,2}}+\frac{1}{k_{1,3}}$ which implies that (since all involved terms are positive and $k_{2,1}=k_{1,2}$):

$$\frac{1}{k_{0,1}}+\frac{1}{k_{1,2}}+\frac{1}{k_{2,3}} \leq \frac{1}{k_{0,2}}+\frac{1}{k_{2,1}}+\frac{1}{k_{1,3}} \quad (48)$$

Finally, equations (43), (45), (47) and (48) show that the minimum of the set $\mathcal{I}$ in (19) is $\frac{1}{k_{0,1}}+\frac{1}{k_{1,2}}+\frac{1}{k_{2,3}}$ and $i=4$ in (20). Based on the above calculations and on [15], equations (43), (45), (47) and (48) show that solution 1 corresponds to the case where the path S-R_1-R_2-D is stronger than the paths S-D, S-R_2-D, S-R_1-D and S-R_2-R_1-D, respectively. The strength of this 3-hop selected path is measured by $\left(\frac{1}{k_{0,1}}+\frac{1}{k_{1,2}}+\frac{1}{k_{2,3}}\right)^{-1}$.

A similar analysis holds for the symmetrical case $P_{0,2} \neq 0$, $P_{1,2} \neq 0$, $P_{1,3} \neq 0$ (path S-R_2-R_1-D rather than S-R_1-R_2-D) by permuting the subscripts 1 and 2. The strength of path S-R_2-R_1-D is $\left(\frac{1}{k_{0,2}}+\frac{1}{k_{2,1}}+\frac{1}{k_{1,3}}\right)^{-1}$ and $i=5$ in (20).

While the cases $i \in \{1,2,3\}$ and $i \in \{4,5\}$ are covered by [15] and the above analysis, respectively, we next prove that all other nontrivial solutions are not feasible.

Solution 2: $P_{0,1} \neq 0$, $P_{1,2} \neq 0$, $P_{2,3} \neq 0$, $P_{1,3} \neq 0$ and the remaining components of $\mathbf{P}$ are zero. We will next prove that this solution which corresponds to simultaneously activating the links reaching D is not feasible. From (37), $\mu_{0,1}=\mu_{1,2}=\mu_{2,3}=\mu_{1,3}=0$ resulting, from (31), (35), (34) and (33), in:

$$\lambda = k_{0,1}e^{-\delta_{0,1}}\left[1+e^{-\delta_{1,2}}e^{-\delta_{2,3}}\right] \doteq k_{0,1}e^{-\delta_{0,1}} \quad (49)$$

$$\lambda = k_{1,2}e^{-\delta_{1,2}}\left[e^{-\delta_{0,1}}e^{-\delta_{2,3}}+e^{-\delta_{1,3}}\right] \doteq k_{1,2}e^{-\delta_{1,2}}e^{-\delta_{1,3}} \quad (50)$$

$$\lambda = k_{2,3}e^{-\delta_{2,3}}\left[e^{-\delta_{1,3}}+e^{-\delta_{1,2}}e^{-\delta_{0,1}}\right] \doteq k_{2,3}e^{-\delta_{2,3}}e^{-\delta_{1,3}} \quad (51)$$

$$\lambda = k_{1,3}e^{-\delta_{1,3}}\left[e^{-\delta_{2,3}}+e^{-\delta_{1,2}}\right] \quad (52)$$

Equations (50)-(52) imply that $\frac{1}{k_{1,3}} = \frac{1}{k_{1,2}}+\frac{1}{k_{2,3}}$. Since this equality among the parameters $k_{1,3}$, $k_{1,2}$ and $k_{2,3}$ that depend on the random path gains does not hold in general, then solution 2 is not feasible. Note that this equality shows the important result that for the power to be split among the links R_1-D and R_1-R_2-D (both emerging from R_1), these links must have exactly the same strength which is impossible following from the randomness of the path gains. In general, one of these links will be stronger than the other implying that one of the links S-R_1-D and S-R_1-R_2-D can be activated at a time. Finally, the non-feasibility of the solution for which $P_{0,2} \neq 0$, $P_{1,2} \neq 0$, $P_{2,3} \neq 0$, $P_{1,3} \neq 0$ can be obtained by symmetry.

Solution 3: $P_{0,1} \neq 0$, $P_{1,2} \neq 0$, $P_{2,3} \neq 0$, $P_{0,2} \neq 0$ and the remaining components of $\mathbf{P}$ are zero. We will next prove that this solution which corresponds to simultaneously activating the links emerging from S is not feasible. From (37), $\mu_{0,1}=\mu_{1,2}=\mu_{2,3}=\mu_{0,2}=0$. Replacing these values in (31), (35), (34) and (32), respectively, results in:

$$\lambda = k_{0,1}e^{-\delta_{0,1}}\left[e^{-\delta_{0,2}}+e^{-\delta_{1,2}}e^{-\delta_{2,3}}\right] \doteq k_{0,1}e^{-\delta_{0,1}}e^{-\delta_{0,2}} \quad (53)$$

$$\lambda = k_{1,2}e^{-\delta_{1,2}}\left[e^{-\delta_{0,1}}e^{-\delta_{2,3}}+e^{-\delta_{0,2}}\right] \doteq k_{1,2}e^{-\delta_{1,2}}e^{-\delta_{0,2}} \quad (54)$$

$$\lambda = k_{2,3}e^{-\delta_{2,3}}\left[1+e^{-\delta_{1,2}}e^{-\delta_{0,1}}\right] \quad (55)$$

$$\lambda = k_{0,2}e^{-\delta_{0,2}}\left[e^{-\delta_{0,1}}+e^{-\delta_{1,2}}\right] \quad (56)$$

Equations (53), (55) and (56) imply that $\frac{1}{k_{0,2}} = \frac{1}{k_{0,1}}+\frac{1}{k_{1,2}}$ (links S-R_2 and S-R_1-R_2 have exactly the same strength) which is not possible. In the same way, the symmetrical case $P_{0,1} \neq 0$, $P_{1,2} \neq 0$, $P_{1,3} \neq 0$ and $P_{0,2} \neq 0$ is not feasible.

Solution 4: $P_{0,1} \neq 0$, $P_{1,2} \neq 0$, $P_{2,3} \neq 0$, $P_{1,3} \neq 0$, $P_{0,2} \neq 0$ and the remaining components of $\mathbf{P}$ are zero (the links emerging from S and the links reaching D are activated simultaneously). From (37), $\mu_{0,1}=\mu_{1,2}=\mu_{2,3}=\mu_{1,3}=\mu_{0,2}=0$. Replacing these values in (31), (35), (34), (33) and

(32), respectively, results in:

$$\lambda = k_{0,1}e^{-\delta_{0,1}}\left[e^{-\delta_{0,2}} + e^{-\delta_{1,2}}e^{-\delta_{2,3}}\right] \doteq k_{0,1}e^{-\delta_{0,1}}e^{-\delta_{0,2}} \tag{57}$$

$$\lambda = k_{1,2}e^{-\delta_{1,2}}\left[e^{-\delta_{0,1}}e^{-\delta_{2,3}} + e^{-\delta_{0,2}}e^{-\delta_{1,3}}\right] \tag{58}$$

$$\lambda = k_{2,3}e^{-\delta_{2,3}}\left[e^{-\delta_{1,3}} + e^{-\delta_{1,2}}e^{-\delta_{0,1}}\right] \doteq k_{2,3}e^{-\delta_{2,3}}e^{-\delta_{1,3}} \tag{59}$$

$$\lambda = k_{1,3}e^{-\delta_{1,3}}\left[e^{-\delta_{2,3}} + e^{-\delta_{1,2}}e^{-\delta_{0,2}}\right] \doteq k_{1,3}e^{-\delta_{1,3}}e^{-\delta_{2,3}} \tag{60}$$

$$\lambda = k_{0,2}e^{-\delta_{0,2}}\left[e^{-\delta_{0,1}} + e^{-\delta_{1,2}}e^{-\delta_{1,3}}\right] \doteq k_{0,2}e^{-\delta_{0,2}}e^{-\delta_{0,1}} \tag{61}$$

Equations (57) and (61) imply that $k_{0,1} = k_{0,2}$ while equations (59) and (60) imply that $k_{1,3} = k_{2,3}$. Both equalities are impossible and the corresponding solution is not feasible.

As a conclusion, the optimal solution corresponds to entirely dedicating the total power to one of the links S-D, S-R_1-D, S-R_2-D, S-R_1-R_2-D and S-R_2-R_1-D according to (19)-(22).

Appendix B
Power Allocation with N Relays

Proposition 2 will be proven by induction. From proposition 1, this induction holds for $N = 2$ relays. Assume that it holds for $N-1$ relays and let us prove that it holds for N relays. While all paths with N or less hops are considered in the $(N-1)$-relay system by induction, the proof reduces to proving proposition 2 for the $(N+1)$-hop paths S-R_1-$\cdots$-R_N-D and S-R_N-$\cdots$-R_1-D of the N-relay system.

Construct the set $\mathcal{S}$ as $\mathcal{S} = \{(0,1),\ldots,(0,N+1),(1,N+1),\ldots,(N,N+1),(1,2),\ldots,(N-1,N)\}$ and define the vector $\mathbf{P}$ as $\mathbf{P} = \left[\{P_{m,n}\}_{(m,n)\in\mathcal{S}}\right]$. We next apply the method of Lagrange multipliers with the solution satisfying the KKT conditions. From (28), we construct the following Lagrangian function:

$$\mathcal{L} = e^{-k_{0,N+1}P_{0,N+1}}G(\mathbf{P}) + \lambda\left(\sum_{(m,n)\in\mathcal{S}} P_{m,n} - 1\right) - \sum_{(m,n)\in\mathcal{S}} \mu_{m,n}P_{m,n} \tag{62}$$

where, from (28), $G(\mathbf{P}) \triangleq e^{k_{0,N+1}P_{0,N+1}}P_e$ and it can be written as:

$$\begin{aligned} G(\mathbf{P}) = {} & \prod_{j=1}^{N} e^{-k_{0,j}P_{0,j}} + \prod_{j=1}^{N} e^{-k_{j,N+1}P_{j,N+1}} \\ & + \sum_{i=1}^{n-1} e^{-k_{i,i+1}P_{i,i+1}}\left(\prod_{j=1}^{i} e^{-k_{0,j}P_{0,j}} \prod_{j=i+1}^{N} e^{-k_{j,N+1}P_{j,N+1}} + \prod_{j=i+1}^{N} e^{-k_{0,j}P_{0,j}} \prod_{j=1}^{i} e^{-k_{j,N+1}P_{j,N+1}}\right) \\ & + \sum_{i=n}^{N-1} e^{-k_{i,i+1}P_{i,i+1}}\left(\prod_{j=1}^{i} e^{-k_{0,j}P_{0,j}} \prod_{j=i+1}^{N} e^{-k_{j,N+1}P_{j,N+1}} + \prod_{j=i+1}^{N} e^{-k_{0,j}P_{0,j}} \prod_{j=1}^{i} e^{-k_{j,N+1}P_{j,N+1}}\right) \end{aligned} \tag{63}$$

At the optimal point $\mathbf{P}$, $\mathcal{L}$ must satisfy the following equation (where $\delta_{m,n} \triangleq k_{m,n}P_{m,n}$):

$$\frac{\partial\mathcal{L}}{\partial P_{0,N+1}} = -k_{0,N+1}e^{-\delta_{0,N+1}}G(\mathbf{P}) + \lambda - \mu_{0,N+1} = 0 \tag{64}$$

and the following N equations ($n = 1,\ldots,N$):

$$\begin{aligned} \frac{\partial\mathcal{L}}{\partial P_{0,n}} = -k_{0,n}e^{-\delta_{0,N+1}} & \left[\prod_{j=1}^{N} e^{-\delta_{0,j}} + \sum_{i=1}^{n-1} e^{-\delta_{i,i+1}} \prod_{j=i+1}^{N} e^{-\delta_{0,j}} \prod_{j=1}^{i} e^{-\delta_{j,N+1}} \right. \\ & \left. + \sum_{i=n}^{N-1} e^{-\delta_{i,i+1}} \prod_{j=1}^{i} e^{-\delta_{0,j}} \prod_{j=i+1}^{N} e^{-\delta_{j,N+1}}\right] + \lambda - \mu_{0,n} = 0 \end{aligned} \tag{65}$$

and the following N equations ($n = 1,\ldots,N$):

$$\begin{aligned} \frac{\partial\mathcal{L}}{\partial P_{n,N+1}} = -k_{n,N+1}e^{-\delta_{0,N+1}} & \left[\prod_{j=1}^{N} e^{-\delta_{j,N+1}} + \sum_{i=1}^{n-1} e^{-\delta_{i,i+1}} \prod_{j=1}^{i} e^{-\delta_{0,j}} \prod_{j=i+1}^{N} e^{-\delta_{j,N+1}} + \right. \\ & \left. \sum_{i=n}^{N-1} e^{-\delta_{i,i+1}} \prod_{j=i+1}^{N} e^{-\delta_{0,j}} \prod_{j=1}^{i} e^{-\delta_{j,N+1}}\right] + \lambda - \mu_{n,N+1} = 0 \end{aligned} \tag{66}$$

as well as the $N-1$ equations ($i = 1,\ldots,N-1$):

$$\begin{aligned} \frac{\partial\mathcal{L}}{\partial P_{i,i+1}} = -k_{i,i+1}e^{-\delta_{0,N+1}}e^{-\delta_{i,i+1}} & \left[\prod_{j=1}^{i} e^{-\delta_{0,j}} \prod_{j=i+1}^{N} e^{-\delta_{j,N+1}} \right. \\ & \left. + \prod_{j=i+1}^{N} e^{-\delta_{0,j}} \prod_{j=1}^{i} e^{-\delta_{j,N+1}}\right] + \lambda - \mu_{i,i+1} = 0 \end{aligned} \tag{67}$$

and the following equation:

$$\frac{\partial\mathcal{L}}{\partial\lambda} = \sum_{(m,n)\in\mathcal{S}} P_{m,n} - 1 = 0 \tag{68}$$

As in appendix A, the KKT conditions are given by:

$$\mu_{m,n}P_{m,n} = 0 \quad ; \quad (m,n)\in\mathcal{S} \tag{69}$$

$$\mu_{m,n} \geq 0 \quad ; \quad (m,n)\in\mathcal{S} \tag{70}$$

Consider the path S-R_1-$\cdots$-R_N-D where the corresponding solution is characterized by $P_{0,1} \neq 0$, $P_{1,2} \neq 0$, $\ldots$, $P_{N-1,N} \neq 0$, $P_{N,N+1} \neq 0$ and the remaining components of $\mathbf{P}$ are zero. From (69), $\mu_{0,1} = 0$. Replacing this value in (65) for $n = 1$ results in:

$$\begin{aligned} \lambda &= k_{0,1}\left[e^{-\delta_{0,1}} + \sum_{i=1}^{N-1} e^{-\delta_{i,i+1}} \prod_{j=1}^{i} e^{-\delta_{0,j}} \prod_{j=i+1}^{N} e^{-\delta_{j,N+1}}\right] \\ &= k_{0,1}\left[e^{-\delta_{0,1}} + e^{-\delta_{0,1}}e^{-\delta_{N,N+1}} \sum_{i=1}^{N-1} e^{-\delta_{i,i+1}}\right] \doteq k_{0,1}e^{-\delta_{0,1}} \end{aligned} \tag{71}$$

In the same way, $\mu_{N,N+1} = 0$ from (69). Replacing this value in (66) for $n = N$ results in:

$$\lambda = k_{N,N+1}\left[e^{-\delta_{N,N+1}} + \sum_{i=1}^{N-1} e^{-\delta_{i,i+1}} \prod_{j=1}^{i} e^{-\delta_{0,j}} \prod_{j=i+1}^{N} e^{-\delta_{j,N+1}}\right]$$
$$= k_{N,N+1}e^{-\delta_{N,N+1}}\left[1+e^{-\delta_{0,1}} \sum_{i=1}^{N-1} e^{-\delta_{i,i+1}}\right] \doteq k_{N,N+1}e^{-\delta_{N,N+1}} \quad (72)$$

Finally, from (69), $\mu_{1,2} = \cdots = \mu_{N-1,N} = 0$ resulting in the following $N-1$ equations form (67) ($i = 1, \ldots, N-1$):

$$\lambda = k_{i,i+1}e^{-\delta_{i,i+1}}\left[e^{-\delta_{0,1}}e^{-\delta_{N,N+1}} + 1\right] \doteq k_{i,i+1}e^{-\delta_{i,i+1}} \quad (73)$$

Now, solving (68), (71), (72) and (73) for $P_{0,1}, P_{1,2}, \ldots, P_{N-1,N}, P_{N,N+1}$ (while eliminating λ) results in the solution given in (22).

We next determine the conditions for which the total power is dedicated to the path S-R_1-$\cdots$-R_N-D. From (70), $\mu_{0,N+1} \geq 0$ implying that (64) can be written as:

$$\mu_{0,N+1} = \lambda - k_{0,N+1}[e^{-\delta_{0,1}} + e^{-\delta_{N,N+1}} + \sum_{i=1}^{N-1} e^{-\delta_{i,i+1}}[e^{-\delta_{0,1}}e^{-\delta_{N,N+1}} + 1]]$$
$$\doteq \lambda - k_{0,N+1}\left[e^{-\delta_{0,1}} + e^{-\delta_{N,N+1}} + \sum_{i=1}^{N-1} e^{-\delta_{i,i+1}}\right] \geq 0 \quad (74)$$

which, from (71), (72) and (73), implies that:

$$\frac{1}{k_{0,1}} + \sum_{i=1}^{N-1} \frac{1}{k_{i,i+1}} + \frac{1}{k_{N,N+1}} \leq \frac{1}{k_{0,N+1}} \quad (75)$$

showing that the inverse-strength of the link S-R_1-$\cdots$-R_N-D is smaller than that of the direct link S-D.

In the same way, (70) implies that $\mu_{0,n} \geq 0$ for $n \neq 1$. Consequently, (65) can be written as (for $n \neq 1$):

$$\mu_{0,n} = \lambda - k_{0,n}\left[e^{-\delta_{0,1}} + \sum_{i=1}^{n-1} e^{-\delta_{i,i+1}} + \sum_{i=n}^{N-1} e^{-\delta_{i,i+1}}e^{-\delta_{0,1}}e^{-\delta_{N,N+1}}\right]$$
$$\doteq \lambda - k_{0,n}\left[e^{-\delta_{0,1}} + \sum_{i=1}^{n-1} e^{-\delta_{i,i+1}}\right] \geq 0 \quad (76)$$

which, from (71) and (73), implies that:

$$\frac{1}{k_{0,1}} + \sum_{i=1}^{n-1} \frac{1}{k_{i,i+1}} \leq \frac{1}{k_{0,n}} \quad (77)$$

showing that the path S-R_1-$\cdots$-R_n is preferred over the path S-R_n.

Finally, (70) implies that $\mu_{n,N+1} \geq 0$ for $n \neq N$. Replacing these inequalities in (66) implies that (for $n \neq N$):

$$\mu_{n,N+1} = \lambda - k_{n,N+1}\left[e^{-\delta_{N,N+1}} + \sum_{i=1}^{n-1} e^{-\delta_{i,i+1}}e^{-\delta_{0,1}}e^{-\delta_{N,N+1}} + \sum_{i=n}^{N-1} e^{-\delta_{i,i+1}}\right]$$
$$\doteq \lambda - k_{n,N+1}\left[e^{-\delta_{N,N+1}} + \sum_{i=n}^{N-1} e^{-\delta_{i,i+1}}\right] \geq 0 \quad (78)$$

which, from (72) and (73), implies that:

$$\sum_{i=n}^{N-1} \frac{1}{k_{i,i+1}} + \frac{1}{k_{N,N+1}} \leq \frac{1}{k_{n,N+1}} \quad (79)$$

showing that the path R_n-$\cdots$-R_N-D is preferred over the path R_n-D.

Now, let us compare the $(N+1)$-hop link S-R_1-$\cdots$-R_N-D with a (N_h+2)-hop link of the form S-R_m-$\cdots$-R_{m+N_h}-D where $N_h \neq N-1$. Adding the inequality in (77) for $n = m$ and the inequality in (79) for $n = m + N_h$ results in:

$$\frac{1}{k_{0,1}} + \sum_{i=1}^{m-1} \frac{1}{k_{i,i+1}} + \sum_{i=m+N_h}^{N-1} \frac{1}{k_{i,i+1}} + \frac{1}{k_{N,N+1}} \leq \frac{1}{k_{0,m}} + \frac{1}{k_{m+N_h,N+1}} \quad (80)$$

Adding the term $\sum_{i=m}^{m+N_h-1} \frac{1}{k_{i,i+1}}$ to both sides of the above inequality results in:

$$\frac{1}{k_{0,1}} + \sum_{i=1}^{N-1} \frac{1}{k_{i,i+1}} + \frac{1}{k_{N,N+1}} \leq \frac{1}{k_{0,m}} + \sum_{i=m}^{m+N_h-1} \frac{1}{k_{i,i+1}} + \frac{1}{k_{m+N_h,N+1}} \quad (81)$$

showing that the inverse-strength of the link S-R_1-$\cdots$-R_N-D is smaller than that of the link S-R_m-$\cdots$-R_{m+N_h}-D.

Finally, let us perform a similar comparison with a (N_h+2)-hop link of the form S-R_{m+N_h}-$\cdots$-R_m-D. Adding the inequality in (77) for $n = m + N_h$ and the inequality in (79) for $n = m$ results in:

$$\frac{1}{k_{0,1}} + \sum_{i=1}^{m+N_h-1} \frac{1}{k_{i,i+1}} + \sum_{i=m}^{N-1} \frac{1}{k_{i,i+1}} + \frac{1}{k_{N,N+1}} \leq \frac{1}{k_{0,m+N_h}} + \frac{1}{k_{m,N+1}} \quad (82)$$

Adding the term $\sum_{i=m}^{m+N_h-1} \frac{1}{k_{i,i+1}}$ to both sides of the above inequality results in:

$$\frac{1}{k_{0,1}} + \sum_{i=1}^{m-1} \frac{1}{k_{i,i+1}} + 3\sum_{i=m}^{m+N_h-1} \frac{1}{k_{i,i+1}} + \sum_{i=m+N_h}^{N-1} \frac{1}{k_{i,i+1}} + \frac{1}{k_{N,N+1}} \leq \frac{1}{k_{0,m+N_h}} + \sum_{i=m}^{m+N_h-1} \frac{1}{k_{i,i+1}} + \frac{1}{k_{m,N+1}} \quad (83)$$

implying that:

$$\frac{1}{k_{0,1}} + \sum_{i=1}^{N-1} \frac{1}{k_{i,i+1}} + \frac{1}{k_{N,N+1}} \leq \frac{1}{k_{0,m+N_h}} + \sum_{i=m}^{m+N_h-1} \frac{1}{k_{i,i+1}} + \frac{1}{k_{m,N+1}} \quad (84)$$

since all involved quantities are positive. Equation (84) shows that the inverse-strength of the link S-R_1-$\cdots$-R_N-D is smaller than that of the link S-R_{m+N_h}-$\cdots$-R_m-D.

Finally, the inequalities in (75), (81) and (84) complete the proof of proposition 2. By symmetry, a similar analysis holds for the link S-R_N-$\cdots$-R_1-D.

REFERENCES

[1] D. Kedar and S. Arnon, "Urban optical wireless communications networks: the main challenges and possible solutions," *IEEE Commun. Mag.*, vol. 42, no. 5, pp. 2 – 7, February 2003.

[2] S. G. Wilson, M. Brandt-Pearce, Q. Cao, and J. H. Leveque, "Free-space optical MIMO transmission with Q-ary PPM," *IEEE Trans. Commun.*, vol. 53, pp. 1402–1412, August 2005.

[3] S. G. Wilson, M. Brandt-Pearce, Q. Cao, and M. Baedke, "Optical repetition MIMO transmission with multipulse PPM," *IEEE J. Select. Areas Commun.*, vol. 23, no. 9, pp. 1901–1910, September 2005.

[4] A. Garcia-Zambrana, C. Castillo-Vazquez, B. Castillo-Vazquez, and A. Hiniesta-Gomez, "Selection transmit diversity for FSO links over strong atmospheric turbulence channels," *IEEE Photon. Technol. Lett.*, vol. 21, pp. 1017 – 1019, July 2009.

[5] C. Abou-Rjeily, "On the optimality of the selection transmit diversity for MIMO-FSO links with feedback," *IEEE Commun. Lett.*, vol. 15, no. 6, pp. 641 – 643, June 2011.

[6] M. Safari and M. Uysal, "Relay-assisted free-space optical communication," *IEEE Trans. Wireless Commun.*, vol. 7, no. 12, pp. 5441 – 5449, December 2008.

[7] M. Karimi and M. Nasiri-Kenari, "Free-space optical communications via optical amplify-and-forward relaying," *J. Lightwave Technol.*, vol. 29, no. 2, pp. 242–2248, January 2011.

[8] ——, "BER analysis of cooperative systems in free-space optical networks," *J. Lightwave Technol.*, vol. 27, no. 24, pp. 5639–5647, December 2009.

[9] C. Abou-Rjeily and A. Slim, "Cooperative diversity for free-space optical communications: Transceiver design and performance analysis," *IEEE Trans. Commun.*, vol. 59, no. 3, pp. 658–663, March 2011.

[10] A. Garcia-Zambrana, C. Castillo-Vasquez, B. Castillo-Vasquez, and R. Boluda-Ruiz, "Bit detect and forward relaying for FSO links using equal gain combining over gamma-gamma atmospheric turbulence channels with pointing errors," *Opt. Express*, vol. 20, no. 15, pp. 16 394 – 16 409, July 2012.

[11] M. R. Bhatnagar, "Performance analysis of decode-and-forward relaying in gamma-gamma fading channels," *IEEE Photon. Technol. Lett.*, vol. 24, no. 7, pp. 545 – 547, April 2012.

[12] ——, "Average BER analysis of differential modulation in DF cooperative communication system over gamma-gamma fading FSO links," *IEEE Commun. Lett.*, vol. 16, no. 8, pp. 1228 – 1231, August 2012.

[13] N. D. Chatzidiamantis, D. S. Michalopoulos, E. E. Kriezis, G. K. Karagiannidis, and R. Schober, "Relay selection protocols for relay-assisted free-space optical systems," *IEEE J. Opt. Commun. Netw.*, vol. 5, no. 1, pp. 4790 –4807, January 2013.

[14] C. Abou-Rjeily, "Achievable diversity orders of decode-and-forward cooperative protocols over gamma-gamma fading FSO links," *IEEE Trans. Commun.*, vol. 61, no. 9, pp. 3919–3930, September 2013.

[15] C. Abou-Rjeily and S. Haddad, "Cooperative FSO systems: Performance analysis and optimal power allocation," *J. Lightwave Technol.*, vol. 29, no. 7, pp. 1058–1065, April 2011.

[16] J. Akella, M. Yuksel, and S. Kalyanaraman, "Error analysis of multihop free-space optical communication," in *Proc. IEEE International Conference on Communications (ICC'5), Seoul, Korea*, May 2005.

[17] T. A. Tsiftsis, H. G. Sandalidis, G. K. Karagiannidis, and N. C. Sagias, "Multihop free-space optical communications over strong turbulence channels," in *Proc. IEEE Int. Conf. on Commun. (ICC'6)*, June 2006.

[18] A. Sendonaris, E. Erkip, and B. Aazhang, "User cooperation diversity. Part I. System description," *IEEE Trans. Commun.*, vol. 51, no. 11, pp. 1927 – 1938, November, 2003.

[19] H. Kuhn and A. Tucker, "Nonlinear programming," in *Proceedings of 2nd Berkeley Symposium. Berkeley: University of California Press*, 1951, p. 481492.

[20] C. Abou-Rjeily, "Performance analysis of selective relaying in cooperative free-space optical systems," *J. Lightwave Technol.*, vol. 31, no. 18, pp. 2965–2973, September 2013.

[21] J. C. Moreira and P. G. Farrell, *Essentials of Error-Control Coding*. Wiley, 2006.

[22] R. R. Parenti, J. M. Roth, J. H. Shapiro, F. G. Walther, and J. A. Greco, "Experimental observations of channel reciprocity in single-mode free-space optical links," *Opt. Express*, vol. 20, no. 19, pp. 21 635–21 644, September 2012.